RSC Advances

PAPER

View Article Online
View Journal | View Issue

Cite this: *RSC Adv.*, 2017, **7**, 9513

Insight into the structure and energy of $Mo_{27}S_xO_y$ clusters†

Xingchen Liu,[a] Dongbo Cao,[a] Tao Yang,[b] Hao Li,[b] Hui Ge,[a] Manuel Ramos,[c] Qing Peng,[d] Albert K. Dearden,[e] Zhi Cao,[f] Yong Yang,[ag] Yong-Wang Li[ag] and Xiao-Dong Wen*[ag]

Received 3rd November 2016
Accepted 24th January 2017

DOI: 10.1039/c6ra26264c

rsc.li/rsc-advances

Oxygen incorporated molybdenum sulfide (MoS_2) nanoparticles are highly promising materials in hydrodesulfurization catalysis, mechanical, electric, and optical applications. We report a systematic theoretical study of the successive oxidation reactions of the $Mo_{27}S_xO_y$ nanoparticles and the reaction network, along with the electronic structure changes caused by the oxygen substitution. The replacement of surface sulfur by oxygen atoms is thermodynamically favorable. Our results indicate that the oxidation on the S edge with 100% and 50% coverage is more favored than on the Mo edge. Meanwhile, it is found that the oxidation on the S edge with 100% coverage has similar replacement ability by oxygen as on the S edge with 50% coverage. Thus, sulfur coverage does not play an important role in the oxidation on the S edge. Further comparison shows that the oxidation on corner sites is more favorable than on edge sites. In addition, the replacement of the bulky sulfur on the Mo edge is equally as favored as those of sulfur on the S edge. This work provides important information on the thermodynamics of the $Mo_{27}S_xO_y$ nanoparticles, and gives new insights into the mechanism of the oxidation of MoS_2 and the sulfidation of MoO_3.

Introduction

With stringent environmental regulations and the declining quality of fossil energy resources, the sulfur level in fuels has renewed the interests in the understanding of the hydrodesulfurization (HDS) mechanism.[1] Molybdenum sulfide catalysts (MoS_x) have been widely used as HDS catalysts for more than 80 years. To understand the HDS mechanism and improve deep HDS catalysts it is necessary to have full insight into the structure and composition of the MoS_x catalysts.

It has been proposed since the 1990s that oxygen plays an important role in the MoS_2 catalyzed HDS reactions. Chary *et al.*[2] found a linear correlation between oxygen chemisorption on MoS_2 and the HDS activity. They thus propose that oxygen chemisorption on MoS_2 and HDS behaves in a similar manner, and that both happen on the coordinatively unsaturated sites (CUS).

The importance of molybdenum oxysulfide clusters is accentuated by the MoS_2 preparation process. It is well known that HDS catalysts are initially prepared from molybdenum oxides by sulfidation. The sulfidation process, which is important for understanding the catalysts structure and HDS mechanism, also involves intermediate state like MoS_xO_y. In 1996, Weber *et al.*[3] studied the sulfidation of MoO_3, and found that the early stage of MoO_3 sulfidation is the transformation to oxysulfides ($MoOS_2$).

In addition, similar to graphene, MoS_2 is known as an important two-dimensional (2D) material of stacks of layers with unique mechanical,[4] electric,[5–7] and optical properties,[8–10] and has become a very promising functional material in nanoelectronics[11] and optoelectronics.[12] As atomic defects such as the oxidation of MoS_2 may be responsible for the variation of its mechanical, electric, optical and catalytic properties,[13] understanding the oxidation process is crucial in improving its performance in all of these aspects. For example, controllable bandgap widening from 1.8 to 2.6 eV was recently achieved through oxidized MoS_2 sheets that are composed of quilted phases of various MoS_xO_y flakes.[14] Oxygen-incorporated MoS_2 nanosheets can be used as catalysts for efficient electrochemical hydrogen evolution[15,16] and oxygen reduction reaction[17] by regulating the electronic structure of MoS_2 with oxygen.

[a]*State Key Laboratory of Coal Conversion, Institute of Coal Chemistry Chinese Academy of Sciences, Taiyuan, Shanxi, 03001 China. E-mail: wxd@sxicc.ac.cn*

[b]*State Key Laboratory of Heavy Oil Processing, China University of Petroleum, Beijing 102249, China*

[c]*Department of Physics and Mathematics, Universidad Autónoma de Cd. Juárez, 450 del Charro Ave. Cd, Juárez, Mexico, 32310*

[d]*Nuclear Engineering and Radiological Sciences, University of Michigan, Ann Arbor, MI 48109-2104, USA*

[e]*Department of Physics, Berea College, Berea, KY 40403, USA*

[f]*Department of Chemistry, University of California, Berkeley, California 94720, USA*

[g]*Synfuels China Co. Ltd., Huairou, Beijing 100195, China*

† Electronic supplementary information (ESI) available. See DOI: 10.1039/c6ra26264c

There have been several studies, earlier on mostly experimental and more recently mostly theoretical, on the oxidation of the MoS_2. The oxidation characteristics of MoS_2 was first reported by Lavik *et al.*[18] with thermogravimetric method and later by Sohn *et al.*[19] with kinetic method. Lince[20,21] used the $MoS_{2-x}O_x$ model with substitutional oxygen and explained the oxidation of MoS_2. In 1999, Fleischauer and Lince[22] compared the oxidation and oxygen substitution in MoS_2 solid film lubricants. They suggested that oxygen atoms are incorporated into the MoS_2 structure. In 2001, Miller *et al.*[23] reported the adsorption of O_2 on MoS_2 catalysts by EXAFS analysis. They found that sulfur atoms are partially substituted by oxygen in MoS_2, and proposed that much of the MoS_2 structure remains unchanged. As they suggested, the bond length of Mo–O is from 1.69 to 1.73 Å. Santosh K. C. *et al.* studied the surface oxidation of monolayer MoS_2 with DFT, and found that the dissociative adsorption of molecular oxygen on the MoS_2 surface is kinetically limited due to the large energy barrier at low temperature.[24] Sen *et al.* also found by DFT that oxygen molecule only weakly interacts with the surface, and the penetration of oxygen atoms and molecules through a defect-free MoS_2 monolayer is prevented by a very high diffusion barrier.[25] Both of the studies imply that the oxidation of MoS_2 happens on the corner or edge atoms with lower coordination number, rather than on the surface (or bulk). The energetics of oxidation of triangular MoS_2 nanoparticles with different S coverages was first reported by Liang *et al.*[26] Using a periodic model, a wide range in the oxidation energy (−0.9 to −2.4 eV) was observed for thee first oxidation step.

Despite these reported works, a systematic study of the thermodynamics of the various oxidation paths and networks are lacking, and the structure of the hexagonal MoS_xO_y nanocluster is still unclear. Previously, we have carried out systematic DFT investigations into the carburization processes of MoS_x clusters to understand their surface structures.[27] In this work, on the basis of the same idea, we report systematically the oxidation of $Mo_{27}S_x$ cluster. The MoS_xO_y clusters are treated with the DFT method. The oxidation processes are performed on the Mo edge (33% sulfur coverage), the S edge (100%, 67% and 50% sulfur coverage) and the bulk $Mo_{27}S_{54}$ cluster, respectively. The oxidation structure and its formation energies are discussed to understand the oxidation processes of $Mo_{27}S_x$ cluster.

The stoichiometric ($Mo_{27}S_{54}$) and non-stoichiometric ($Mo_{27}S_x$) clusters were used to model the MoS_2 surfaces. The structures of $Mo_{27}S_{54}$ (**I**) with 0% sulfur coverage on Mo edge and 100% sulfur coverage on S edge, $Mo_{27}S_{56}$ (**II**) with two bridge S atoms on Mo edge (33% sulfur coverage on Mo edge), $Mo_{27}S_{51}$ (**III**) with three bridge S atoms on S edge (50% sulfur coverage on S edge) are shown in Fig. 1. The transformation between various molybdenum sulfide clusters and the corresponding reaction energies are summarized in eqn (1) and (2). In our previous study,[28] we reported various $Mo_{27}S_x$ clusters. On the basis of eqn (1) and (2), the formation of $Mo_{27}S_{56}$ (**II**) and $Mo_{27}S_{51}$ (**III**) is exothermic by 0.19 and 4.61 eV, respectively.

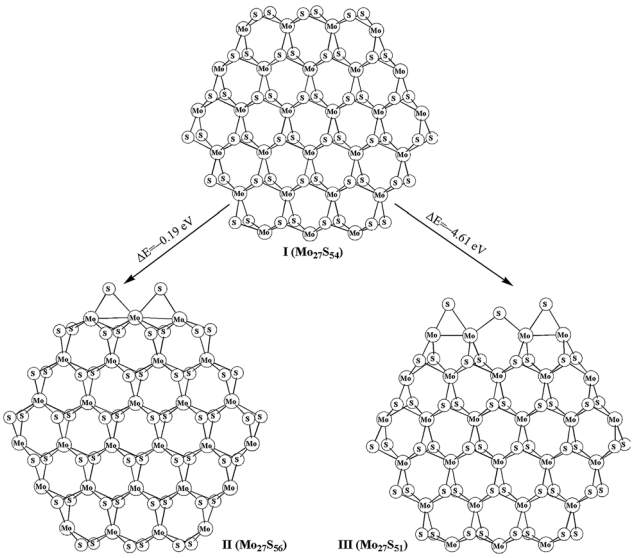

Fig. 1 Optimized different $Mo_{27}S_x$ cluster models.

$$Mo_nS_m + xH_2S = Mo_nS_{m+x} + xH_2$$
(adding sulfur to Mo edge), $\Delta E_0(Mo) = [E(Mo_nS_{m+x}) + E(xH_2)] - [E(Mo_nS_m) + E(xH_2S)]$ (1)

$$Mo_nS_m + xH_2 = Mo_nS_{m-x} + xH_2S$$
(deleting sulfur from S edge), $\Delta E_0(S) = [E(Mo_nS_{m-x}) + E(xH_2S)] - [E(Mo_nS_m) + E(xH_2)]$ (2)

In this work, we used the atom formation energy in eqn (3) to investigate the oxidation process, in which we have used atomic oxygen and sulfur as references. On the basis of eqn (3), the more negative the atom formation energies, the more favorable the process. To address the possibility of other oxidation species instead of atomic oxygen, we also used the following equation for calculating the formation energy: $Mo_{27}S_x + nO_2 = Mo_{27}S_{x-n}O_n + \frac{1}{2}nSO_2 + \frac{1}{2}nS$. Compared to eqn (3), there is only a quantitative difference by −1.71 eV per oxygen ($\frac{1}{2}nS + nO_2 = nO + \frac{1}{2}SO_2$), which does not change our qualitative conclusion that the oxygen process is exothermic. In additon, it is convenient for comparing with carburization process with using the atomic formation energy.

$$Mo_{27}S_x + nO = Mo_{27}S_{x-n}O_n + nS,\ \Delta E_f = [E(Mo_{27}S_{x-n}O_n) + nE(S)] - [E(Mo_{27}S_x) + nE(O)]$$ (3)

Computational section

All calculations are performed with the program package DMol[29] in the Materials Studio of Accelrys Inc. In DMol[29] the physical wave functions are expanded in terms of accurate numerical basis sets.[29–31] We have used the doubled numerical basis set with polarization functions for other elements (DNP), while effective core potential (ECP)[32] is used for molybdenum. The generalized gradient corrected functional by Perdew and Wang (GGA-PW91)

is used[33] and the medium quality mesh size is used for the numerical integration. The tolerances of energy, gradient and displacement convergence are 2×10^{-5} au, 4×10^{-3} au Å^{-1}, 5×10^{-3} Å, respectively. The real space cutoff of atomic orbitals is set at 5.5 Å, and a Fermi smearing of 0.0005 was used to count the orbital occupancy. All structures are fully optimized without any constrain. Vibrational frequency calculations were used to confirm the local minima. The atomic position of $Mo_{27}S_x$ cluster and corresponding inputs used are shown in ESI.†

Results and discussion

1. Oxidation on Mo edge

The oxidation processes and structures are shown in Fig. 2. The formation energy for $Mo_{27}S_{56}$ (**II**) of −13.04 eV is obtained by using S atom as the reactant ($Mo_{27}S_{54} + 2S = Mo_{27}S_{56}$). The first replacement step from $Mo_{27}S_{56}$ (**II**) to form $Mo_{27}S_{55}O$ (**1**) is −1.93 eV, and the second step from **1** to $Mo_{27}S_{54}O_2$ (**2**) is also −1.93 eV. The two steps have the same formation energies, and are both exothermic processes, indicating that the sulfur and oxygen atoms on the Mo edge are roughly independent. A direct oxidation on the Mo edge of $Mo_{27}S_{54}$ (**I**) is also favored thermodynamically by −16.91 eV. In addition, it is obvious that oxidation is more favored than sulfidation on the Mo edge with 0% sulfur coverage. In other words, the O atom is more favored than S atom to be bonded with Mo. Other than that, by comparing oxidation with the carburization process of MoS_2 in the literature,[5] it is clear that the oxidation is also more favorable than carburization on the Mo edge.

Liang *et al.*[26] also studied the oxidation of MoS_2 edges with DFT, and is worth comparison in the discussion. To begin with, they studied the edge oxidation of triangular MoS_2 clusters, while our works studies the edge oxidation of hexagonal MoS_2 clusters. Experimentally,[34,35] both triangle-shaped and hexagonal MoS_2 nanoclusters were observed as stable forms of existence. Because of the difference in topology, coordination environment, and the electronic structures from quantum size effect, the oxidations of the edges of different shaped MoS_2 clusters are different. Indeed, their structures of Mo edge are covered with 0%, 50%, and 100% sulfur, while our Mo edge is covered with 33% sulfur.

Second, their work only studied the first oxidation step, equivalent to the step of **II** ($Mo_{27}S_{56}$) to **1** ($Mo_{27}S_{55}O$) in our studies in Fig. 2. Interestingly, comparing the oxidation energies on Mo edge, our value of −1.93 eV at 33% coverage is well within the case of −1.5 eV, −1.6 eV and −1.8 eV at 0% coverage and the case of −2.1 eV and −2.4 eV at 50% coverage in Liang's work.

We have tried to explain this energetic difference among oxidation, carburization and sulfidation by using the bonding energies, but the related experimental data for Mo–S bond(s) is not available. However, on the basis of the Pauling's rule for estimating bond energies,[36] the estimated Mo–S bond energy is around 433 kJ mol^{-1}. The Mo–O and Mo–C bond energy is 560.2 ± 20.9 and 481 ± 15.9 kJ mol^{-1} from the available experimental data,[37] respectively. Thus the estimated Mo–S bond energy is much lower than the Mo–O and Mo–C values, and Mo–O has the highest bond energy. This gives a qualitative conclusion that Mo–O bond is stronger than Mo–S or Mo–C bond, and therefore the formation of Mo–O bonds is energetically more favored than Mo–S and Mo–C bonds. This is in agreement with the local electronic density of states (EDOS) study in the literature,[26] which states that the oxidation of MoS_2 is the result of local competition of binding energy of the covalent bonds.

The changes of the oxidation surface structure (Mo–Mo distance and Mo–S distance) are shown in Fig. 2. The Mo–Mo bond length is 3.134 and 2.951 Å in $Mo_{27}S_{54}$ (**I**) and $Mo_{27}S_{56}$ (**II**), respectively, while it is shorter in **2** (2.832 Å). It is worth noting that the Mo–Mo distance in $Mo_{27}S_{54}$ (**I**) matches very well with the experimental value of 3.15 ± 0.1 Å of the same hexagonal single-layer MoS_2 nanocluster from STM.[36] The Mo–C distances are 1.875 and 2.174 Å. Meanwhile, the distance (2.413 Å) of corner Mo atom to corner S atom is longer than that of in $Mo_{27}S_{54}$ cluster (2.331 Å), as shown in Fig. 2. Substitution of the S atoms on the edge with O atoms drew the Mo atoms that they are connecting with closer by about 0.09 Å, making the structure more "compact" on the edge. However, the remaining Mo–S bonds in the bulk are slightly elongated, because O has more electron negativity than S and the Mo–O bonds are stronger than the Mo–S bonds. Similar structural distortions are also found in the oxidation of other edges in the following sections.

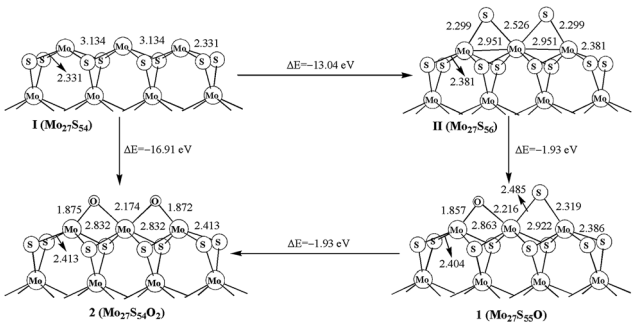

Fig. 2 Oxidation on Mo edge.

2. Oxidation on 100% covered S edge

For replacing one S atom in $Mo_{27}S_{54}$ (**I**) by oxygen, there are two possible structures. Structure **3** and **4** with one corner S atom and one edge S atom replaced are shown in Fig. 3, respectively. From formation energy, both replacements are exothermic. The replacement of the corner S atom (**3**, −2.46 eV) is more favored than the edge S atom (**4**, −2.35 eV). Both of the oxidation are more easier than that of the S edge with 100% sulfur coverage (−1.3 eV for corner, and −1.9 eV for edge) on the triangular MoS_2 cluster reported by Liang *et al.*[26] This can be ascribed to the different chemical environment of the oxidation sites on the hexagonal and triangle-shaped clusters. From bond length parameters in Fig. 3, one can see that the Mo(c)–O and Mo(o)–O bond lengths are 1.875 and 2.044 Å in **3**, respectively. In **4**, the Mo(o)–O bond lengths are 1.948 and 1.977 Å. In carburization processes, C═S species are formed. However, there are not O═S species in oxidation processes. That is, the distance of the

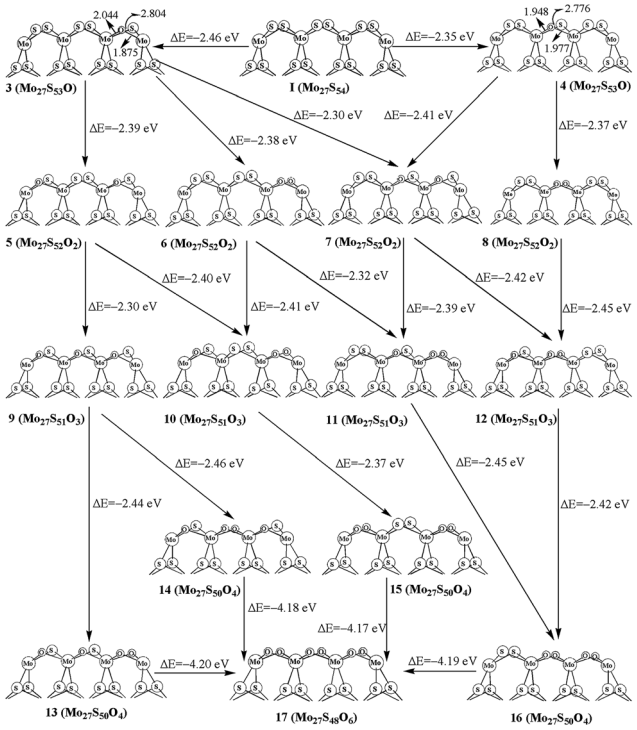

Fig. 3 Oxidation on S edge with 100% sulfur coverage.

O atom and the neighbor S atom is 2.804 Å in **3** and 2.776 Å in **4**, and is longer than C═S (from 1.790 to 1.826 Å) in carburization structures. This shows the difference in structures between carburization and oxidation.

For replacing two sulfur atoms on 100% covered S edge, there are four structures (**5**, **6**, **7** and **8**). As shown in Fig. 3, **5** has two corner S atoms replaced, while **7** has one corner and one edge S atoms replaced. **6** and **8** have two oxygen atoms replacement at the same corner and edge, respectively. The formation energy shows that corner site replacement at the different corner (**5**, −2.39 eV) and at the same corner (**6**, −2.38 eV) is more favored than those at edge (**7**, −2.30 eV). Also, stating from **4**, the corner site replacement (**7**, −2.41 eV) is more favorable than the edge site replacement (**8**, −2.38 eV). It indicates that the oxidation at corner site on the surface is more favored.

As shown in Fig. 3, there are four structures for replacing three sulfur atoms by carbons atoms (**9**, **10**, **11** and **12**). In **10** and **11**, there are two corner oxygen atoms and one single oxygen atom on the corner or edge. Structure **12** has two edge oxygen atoms and one single corner oxygen atom. However, **9** has three single oxygen atoms on the same side of the molecule plane. From the calculated formation energy, one can see that the replacement at corner sites is generally more favored than at the edge. In addition, we have also computed the four-oxygen (**13**, **14**, **15** and **16**) and full oxygen (**17**) replacement. All these processes are favored thermodynamically.

3. Oxidation on 50% covered S edge

The oxidation processes on 50% covered S edge in $Mo_{27}S_{51}$ (**III**) is illustrated in Fig. 4. For one oxygen replacement, there are

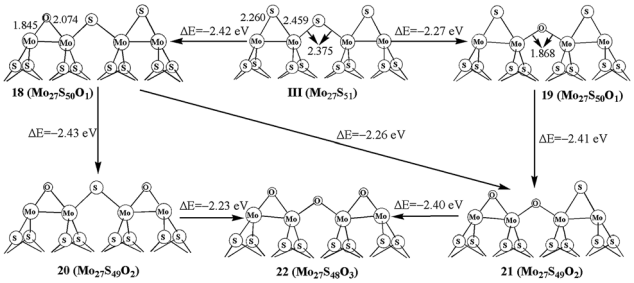

Fig. 4 Oxidation on S edge with 50% sulfur coverage.

two possible structures (**18** and **19**): one with a corner S atom replaced (**18**) and one with an edge S atom replaced (**19**), as shown in Fig. 4. The formation energy difference shows that corner oxygen (**18**, −2.42 eV) can be more easily formed than the edge one that bridges two Mo atoms (**19**, −2.27 eV). Similar preference for corner oxidation is observed at the additional S replacement in **20** (−2.43 eV) and **21** (−2.26 eV) from structure **18**. This is different from the case in triangle-shaped MoS_2,[26] where the oxidation corner oxidation (−2.3 eV) is easier than the edge oxidation (−2.1 eV). In addition, the formation of **22** with full replacement (−2.40 eV) from structure **21** is easier than that of from **20** (−2.23 eV). By comparing with carburization on same edge, the carburization at the edge site is more favorable than at the corner, and is different with oxidation processes. This indicates the difference between carburization and oxidation processes.

4. Oxidation of the bulky S in $Mo_{27}S_{54}$

As shown in the above studies, the oxidation of surface sulfur on Mo edge and S edge has been discussed. It is worth noting of the possibility of replacing the bulky sulfur. As shown in Fig. 5, there are four types of bulky sulfur atoms in $Mo_{27}S_{54}$ (**I**). The first bulky sulfur is S_1 to the Mo edge, and the second type is S_2 close to the S edge. The third type is S_3, which is one line deeper than S_1, and the fourth type is S_4, which is one line deeper than S_2. These symbolic bulky S atoms are also used in carburization processes.

The replacement of S_1 is easier than that of S_2, as indicated by the formation energy of **23** (−2.38 eV) and **24** (−2.32 eV). Comparably the replacement of S_3 and S_4 is very difficult (**25**, −2.28 eV, and **26**, −2.17 eV, respectively). Therefore, S_1 is the type of bulky sulfur, which can be replaced most easily. Like previous work on carburization, our results also indicate that the carburization of bulky sulfur on the Mo edge is as equally favored as those of sulfur on the S edge.

We further report the replacements of multiple S_1 atoms. Structure **27** and **28** with two S_1 atoms replaced on different planes and on the same plane are shown in Fig. 6, respectively. The formation energy shows that replacing two S_1 atoms at the same plane (**28**, −2.42 eV) is more favored than that at different planes (**27**, −2.31 eV). The same result is also shown in **29**. As shown in Fig. 6, the formation of **29** from structure **27** is more easily than that of from **28**. In addition, the replacement of four S_1 atoms (**30**, −2.27 eV) is also exothermic. As comparison, the

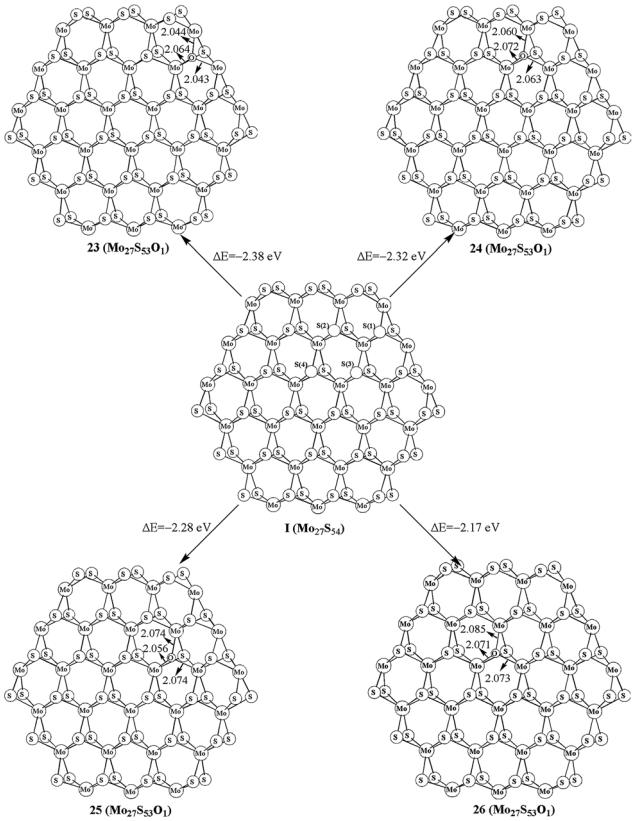

Fig. 5 Oxidation on the bulk of $Mo_{27}S_{54}$.

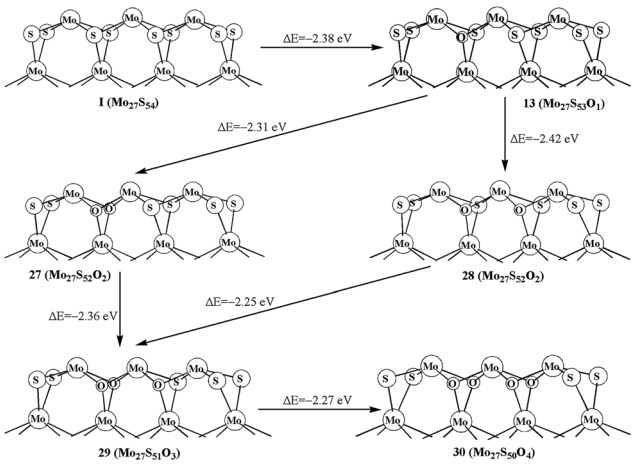

Fig. 6 Oxidation on the bulky S_1 atoms of $Mo_{27}S_{54}$.

oxidation of the bulky S in triangle-shaped MoS_2 cluster is exothermic by only −1.4 eV to −1.7 eV, except for the one (−2.3 eV) that is close to the corner of cluster with 100% sulfur coverage.[26]

5. The effect of oxidation on the density of states of $Mo_{27}S_{54}$

To provide a better understanding of the oxidation process, the electronic structure analysis of the $Mo_{27}S_{54-x}O_x$ clusters are presented here. To start with, the density of states (DOS) of the whole clusters is calculated (Fig. 7, left). There are three major peaks in the DOS of the $Mo_{27}S_{54-x}O_x$ clusters. The DOS at the energy level of −8.4 to 3.3 eV is mainly filled with the 4d electrons of Mo, 3p electrons of S, and 2p electrons of O. The peak at about −12 eV is identified with the 3s electrons of S and the 5s electrons of Mo, and the peak at about −19 eV corresponds to the 2s electrons of O.

With the substitution, the O (2s) peak at −19 eV intensifies gradually, and a small blue shift is observed. The S (3s) and Mo (5s) peak at −12 eV weakens and shifts to lower energy. The large peak from −8.4 eV to 3.3 eV has a shift in energy to lower values. However, the intensity and area of the peak does not change significantly. This shows that the during oxidation, the overlap of the Mo 4d electrons with the S 3p electrons can be roughly replaced by the overlap of the Mo 4d electrons with the O 2p electrons, and that the total number of electrons involved in these two types of bonding remain unchanged.

It is known that MoO_3 is a semiconductor with band gap of around 3.1 eV,[38] while MoS_2 has a band gap of 1.9 eV.[38] By intuition, we would think that the oxidation of $Mo_{27}S_{54}$ will lead to the increase of the HOMO–LUMO gap. However, interestingly, this is not the case as shown in Fig. 7 (right). On the contrary, we observe a general decrease of the HOMO–LUMO gap of the $Mo_{27}S_{54-x}O_x$ clusters with oxidation. This difference in the trend can be attributed to the quantum confinement effect of the nanoscale clusters. In fact, all the $Mo_{27}S_{54-x}O_x$ clusters studied show strong metallic nature with very small HOMO–LUMO gaps. Besides, oxidation increases the metallic nature of the $Mo_{27}S_{54}$ cluster. The HOMO orbital of all clusters has energy of about −5.2 eV. Therefore, the valence band regions of the clusters are from −8.4 eV to −5.2 eV. The width of the valence band is about 3.2 eV, and is significantly smaller than that of either bulk MoO_3 or MoS_2 (about 6 eV).

To further illuminate the trend of changes of the electronic structures of the local sites, the local electronic density of states (LDOS) of an edge Mo atom and the 4 neighboring S atoms before and after substitution are plotted in **Fig. 8**, with each graph representing a different oxidation state. Before substitution, the four S atoms (labeled as a–f) of interest in the $Mo_{27}S_{54}$ cluster are indistinguishable with exactly the same LDOS (**Fig. 8a**). After substitution, the peak at −19 eV appears clearly for O and Mo and slightly for the other three S atoms (**Fig. 8b**). The latter fact suggests that after oxidation, there is considerable overlap between O 2s and Mo orbitals, but only a small amount of overlap

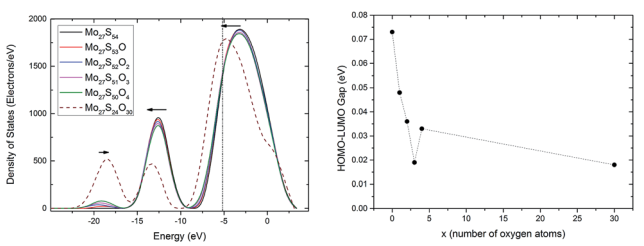

Fig. 7 (Left) Density of states of the $Mo_{27}S_{54-x}O_x$ clusters; the vertical line represents the HOMO orbital energy of the clusters; (right) the HOMO–LUMO gap of the $Mo_{27}S_{54-x}O_x$ cluster subjected to oxidation.

between O 2s and S orbitals. Another proof of the latter statement is that, after oxidation, the O atom includes some electrons from S, as shown at the peak of −12 eV. This is different from the case in the oxidation of the edge of triangular MoS_2 with 100% S coverage reported in literature,[26] where no overlap was observed at all between O 2s and the S orbitals. The further substitution of S by O has almost no effect on the bonding of the previously added O, as Fig. 8c to e shows. Comparing Fig. 8e to f, the oxidation of the rest of all the edge S atoms only affected the valence band region (−8.4 eV to −5.2 eV), mainly related to the Mo 4d electrons and the conduction band (−5.2 eV to 3.3 eV). The core level regions are almost not affected.

6. Vibrational frequencies

MoS_2 is a semiconductor and have the absorption edge in near-IR region. Previous study[39] have shown that the absorption spectra depend strongly on the size of the system. However, the IR spectra of MoS_2 nanoparticles with size similar to the clusters used in this work are not available in the literature.

The IR spectra of all the clusters before and after oxidation are very similar, in agreement with the finding that it's absorption is only slightly sensitive to oxidation suggested in the literature.[39] Because of the broken symmetry of the clusters compared to the bulk, concerted vibrational modes of atoms in the cluster may not match very well with the experimental IR with large single layers of MoS_2. However, some agreements were identified.

Taking structure **27** in Fig. 6 as an example, the calculated IR spectra show a broad region between 420 cm^{-1} and 520 cm^{-1}, which correspond to the Mo–S vibrations of MoS_2 (480 cm^{-1}) reported in experiment.[40] For oxygen in the bulk, another broad peak appears at about 600 cm^{-1} to 650 cm^{-1}, with Mo–O symmetric stretching contained in the vibrational mode with frequency of 609 cm^{-1}. The asymmetric stretching of Mo–O appears at 726 cm^{-1}.

For terminal Mo═O vibrations, IR calculation on structure **10**, for example, show Mo═O asymmetric stretching at 909 cm^{-1} to 914 cm^{-1} and symmetric stretching at 691 cm^{-1}, in agreement with the experimental value[41] of 941 cm^{-1} and 693 cm^{-1}, respectively.

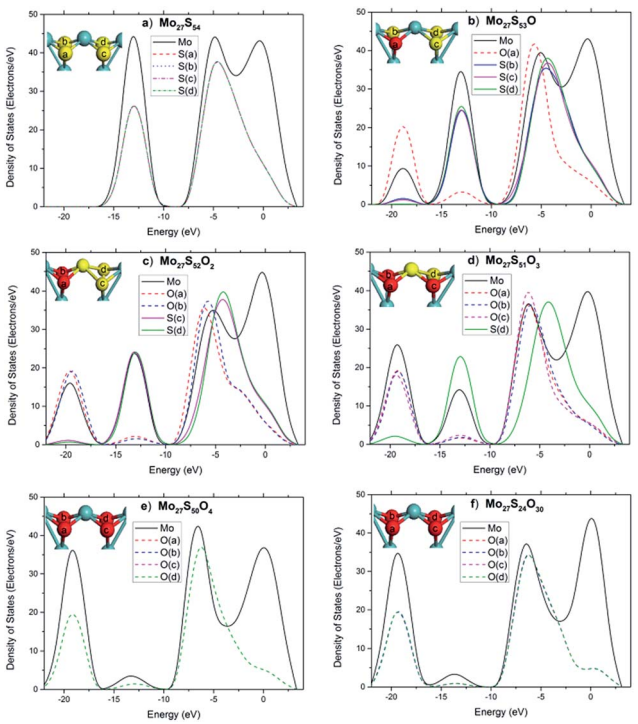

Fig. 8 LDOS of the tetra-coordinated Mo atom on the edge of the $Mo_{27}S_{54-x}O_x$ cluster.

Conclusions

We have carried out systematic investigations into the replacement of the surface sulfur on Mo edge and S edge as well as bulky sulfur to understand the oxidation processes of MoS_x. On these surfaces, the replacement of surface sulfur by the oxygen atoms is thermodynamically favorable.[22,24,26] By comparing the oxidation processes on the surfaces of different sulfur coverage, our results indicate that the oxidation on the S edge with 100% and 50% coverage is more favored than on the Mo edge. Meanwhile, it is found that the oxidation on the S edge with 100% coverage have similar replacement ability by oxygen as on the S edge with 50% coverage. Thus, sulfur coverage does not play important role in the oxidation on the S edge. Further comparison shows that the oxidation on corner sites is more favorable than on edge sites. In addition, the replacement of the bulky sulfur on the Mo edge is equally as favored as those of sulfur on the S edge. If we consider only the replacement of the S atoms by O, instead of a large variation (−0.9 to −2.4 eV) in the oxidation energy reported by Liang[26] with plane-wave basis, we find that the range of the oxidation energy is rather narrow (−1.9 eV to −2.4 eV) for MoS_x. This is probably due to the weakness of the plane-wave model in treating finite clusters. The $Mo_{27}S_xO_y$ nanoclusters have unique electronic properties compared to the bulk. The width of its valence band is about 3.2 eV, and is much smaller than that of either bulk MoO_3 or MoS_2. The electronic structure of the $Mo_{27}S_xO_y$ nanoclusters can be easily tuned by the substitution of S atoms with O atoms.

By comparing with carburization processes on these surfaces, we find that for Mo edge the oxidation is much easier than carburization from their atomic formation energy. There is a large difference of formation energy (−1.93 *vs.* −0.77 eV) between oxidation and carburization. By comparing with carburization and sulfidation, it is shown that oxidation is more favored than carburization and sulfidation on Mo edge. However, on the S edge with 100% coverage, there are only small differences in oxidation and carburization ability, although they have different surface structures. As one can see, there are C═S and C═C species in carburization processes, while O═S and O═O species are not formed in oxidation processes. This is reflected by the difference between carburization and oxidation in experiments. Further, we find that the oxidation on the 100% and 50% covered S edge have similar reaction energy, while the carburization on the 100% covered S edge is more favored than on the 50% covered S edge. This shows that the carburization

depends on the effect of coverage, but oxidation does not. For bulky S, the oxidation and carburization of the bulky sulfur on the Mo edge is equally favored as those of sulfur on S edge. This suggests that the bulky sulfur probably plays important roles in oxidation. From these calculations, we can get the following information:

(1) The S atoms on S edge and in the bulk can be oxidized first. Also, the oxidation on S edge does not depend on its coverage. Following this, the S atoms on Mo edge will be oxidized next. Since the frictional resistance between the MoS_2 layers is determined by the van de Waals forces of the S atoms, the substitution of the S atoms by O would inevitably affect its performance as lubricant. Our results suggests that the capability of MoS_2 lubricants has link with not only the oxidation of the S edge but also bulky at certain degree.

(2) From these results, we can know about some sulfidation process of MoO_3 (precursor). As the opposite processes to oxidation, it is very difficult to sulfurize the O atoms on S edge and bulky, due to the high cost in energy. That is to say, the sulfidation of MoO_3 is probably determined by the sulfidation on S edge and the bulk. Although these studies provides important information on the thermodynamic aspects of the oxidation of MoS_2, further experimental and theoretical studies are needed to understand structure and other property of the oxidized material.

Acknowledgements

The authors are grateful for the financial support from the National Natural Science Foundation of China (No. 21473229, No. 91545121, No. 21603252, and No. 21473231), No. 201601D021048 from the Shanxi Province Science Foundation for Youth, and from Synfuels China, Co. Ltd. We also acknowledge the innovation foundation of Institute of Coal Chemistry, Chinese Academy of Sciences, National Thousand Young Talents Program of China, Hundred-Talent Program of Chinese Academy of Sciences and Shanxi Hundred-Talent Program.

Notes and references

1 H. H. Gary, G. E. Handwerk and M. J. Kaiser, *Petroleum Refining: Technology and Economics*, CRC Press, 5th edn, 2007.
2 K. V. R. Chary, H. Ramakrishna, K. S. Rama Rao, G. Murali Dhar and P. Kanta Rao, *Catal. Lett.*, 1991, **10**, 27–33.
3 T. Weber, J. C. Muijsers, J. H. M. C. van Wolput, C. P. J. Verhagen and J. W. Niemantsverdriet, *J. Phys. Chem.*, 1996, **100**, 14144–14150.
4 F. J. Clauss, *Solid Lubricants and Self-Lubricating Solids*, Academic Press, New York, 1972.
5 B. Radisavljevic, A. Radenovic, J. Brivio, V. Giacometti and A. Kis, *Nat. Nanotechnol.*, 2011, **6**, 147–150.
6 M. M. Perera, M.-W. Lin, H.-J. Chuang, B. P. Chamlagain, C. Wang, X. Tan, M. M.-C. Cheng, D. Tománek and Z. Zhou, *ACS Nano*, 2013, **7**, 4449–4458.
7 S. Kim, A. Konar, W.-S. Hwang, J. H. Lee, J. Lee, J. Yang, C. Jung, H. Kim, J.-B. Yoo, J.-Y. Choi, Y. W. Jin, S. Y. Lee, D. Jena, W. Choi and K. Kim, *Nat. Commun.*, 2012, **3**, 1011.
8 K. F. Mak, K. He, J. Shan and T. F. Heinz, *Nat. Nanotechnol.*, 2012, **7**, 494–498.
9 H. Zeng, J. Dai, W. Yao, D. Xiao and X. Cui, *Nat. Nanotechnol.*, 2012, **7**, 490–493.
10 T. Cao, G. Wang, W. Han, H. Ye, C. Zhu, J. Shi, Q. Niu, P. Tan, E. Wang, B. Liu and J. Feng, *Nat. Commun.*, 2012, **3**, 887.
11 J. Andrés, S. Berski, M. Feliz, R. Llusar, F. Sensato and B. Silvi, *C. R. Chim.*, 2005, **8**, 1400–1412.
12 Q. H. Wang, K. Kalantar-Zadeh, A. Kis, J. N. Coleman and M. S. Strano, *Nat. Nanotechnol.*, 2012, **7**, 699–712.
13 J. Hong, Z. Hu, M. Probert, K. Li, D. Lv, X. Yang, L. Gu, N. Mao, Q. Feng, L. Xie, J. Zhang, D. Wu, Z. Zhang, C. Jin, W. Ji, X. Zhang, J. Yuan and Z. Zhang, *Nat. Commun.*, 2015, **6**, 6293.
14 S. H. Song, B. H. Kim, D.-H. Choe, J. Kim, D. C. Kim, D. J. Lee, J. M. Kim, K. J. Chang and S. Jeon, *Adv. Mater.*, 2015, **27**, 3152–3158.
15 J. Guo, F. Li, Y. Sun, X. Zhang and L. Tang, *J. Power Sources*, 2015, **291**, 195–200.
16 J. Xie, J. Zhang, S. Li, F. Grote, X. Zhang, H. Zhang, R. Wang, Y. Lei, B. Pan and Y. Xie, *J. Am. Chem. Soc.*, 2013, **135**, 17881–17888.
17 H. Huang, X. Feng, C. Du, S. Wu and W. Song, *J. Mater. Chem. A*, 2015, **3**, 16050–16056.
18 M. T. Lavik, T. M. Medved and G. D. Moore, *ASLE Trans.*, 1968, **11**, 44–55.
19 H. Y. Sohn and D. Kim, *Metall. Trans. B*, 1988, **19**, 973–975.
20 J. R. Lince, *J. Mater. Res.*, 1990, **5**, 218–222.
21 J. R. Lince, M. R. Hilton and A. S. Bommannavar, *Surf. Coat. Technol.*, 1990, **43–44**(2), 640–651.
22 P. D. Fleischauer and J. R. Lince, *Tribol. Int.*, 1999, **32**, 627–636.
23 J. T. Miller, C. L. Marshall and A. J. Kropf, *J. Catal.*, 2001, **202**, 89–99.
24 K. C. Santosh, R. C. Longo, R. M. Wallace and K. Cho, *J. Appl. Phys.*, 2015, **117**, 135301.
25 H. S. Sen, H. Sahin, F. M. Peeters and E. Durgun, *J. Appl. Phys.*, 2014, **116**, 083508.
26 T. Liang, W. G. Sawyer, S. S. Perry, S. B. Sinnott and S. R. Phillpot, *J. Phys. Chem. C*, 2011, **115**, 10606–10616.
27 X.-D. Wen, Z. Cao, Y.-W. Li, J. Wang and H. Jiao, *J. Phys. Chem. B*, 2006, **110**, 23860–23869.
28 X.-D. Wen, T. Zeng, Y.-W. Li, J. Wang and H. Jiao, *J. Phys. Chem. B*, 2005, **109**, 18491–18499.
29 B. Delley, *J. Chem. Phys.*, 1990, **92**, 508–517.
30 B. Delley, *J. Phys. Chem.*, 1996, **100**, 6107–6110.
31 B. Delley, *J. Chem. Phys.*, 2000, **113**, 7756–7764.
32 D. Andrae, U. Häußermann, M. Dolg, H. Stoll and H. Preuß, *Theor. Chim. Acta*, 1990, **77**, 123–141.
33 J. P. Perdew and Y. Wang, *Phys. Rev. B: Condens. Matter Mater. Phys.*, 1992, **45**, 13244–13249.
34 J. V. Lauritsen, J. Kibsgaard, S. Helveg, H. Topsoe, B. S. Clausen, E. Laegsgaard and F. Besenbacher, *Nat. Nanotechnol.*, 2007, **2**, 53–58.

35 J. V. Lauritsen, M. V. Bollinger, E. Laegsgaard, K. W. Jacobsen, J. K. Norskov, B. S. Clausen, H. Topsoe and F. Besenbacher, *J. Catal.*, 2004, **221**, 510–522.
36 L. Pauling, *The Nature of the Chemical Bond and the Structure of Molecules and Crystals*, Cornell University Press, New York, 1960.
37 D. R. Lide, *Handbook of Chemistry and Physics*, CRC Press, 84th edn, 2004.
38 *Gmelin Handbook of inorganic and organometallic chemistry. [System number 45]. Ge–Organogermanium compounds*, Springer-Verlag, Berlin, New York, 8th edn, 1993.
39 C. B. Roxlo, M. Daage, A. F. Ruppert and R. R. Chianelli, *J. Catal.*, 1986, **100**, 176–184.
40 S. Liu, X. Zhang, H. Shao, J. Xu, F. Chen and Y. Feng, *Mater. Lett.*, 2012, **73**, 223–225.
41 G. Nagaraju, C. Tharamani, G. Chandrappa and J. Livage, *Nanoscale Res. Lett.*, 2007, **2**, 461.